Macromolecules

ARTICLE

pubs.acs.org/Macromolecules

Origin of the Difference between Branching in Acrylates Polymerization under Controlled and Free Radical Conditions: A Computational Study of Competitive Processes

Dominik Konkolewicz,[†] Stanislaw Sosnowski,[‡] Dagmar R. D'hooge,[†,§] Ryszard Szymanski,[‡] Marie-Françoise Reyniers,[§] Guy B. Marin,[§] and Krzysztof Matyjaszewski*[,†]

[†]Center for Macromolecular Engineering, Department of Chemistry, Carnegie Mellon University, 4400 Fifth Avenue, Pittsburgh, Pennsylvania 15213, United States

[‡]Center of Molecular and Macromolecular Studies of Polish Academy of Sciences, Sienkiewicza 112, 90-363 Lodz, Poland

[§]Laboratory for Chemical Technology, Ghent University, Krijgslaan 281 (S5), Gent, Belgium

Supporting Information

ABSTRACT: A computational study of the branching in polyacrylates is performed for both atom-transfer radical polymerization (ATRP) and free radical polymerization (FRP). In both cases the secondary radical formed can transfer to polymer to generate a tertiary radical, which can propagate with monomer to re-form the secondary species. The critical difference between these two processes is that the exchange between tertiary and secondary species is supplemented in ATRP by additional activation and deactivation reactions for both the secondary and tertiary species. This leads to a competition between the activation−deactivation and exchange processes in ATRP, while there is no such competition in FRP. This introduces the idea of competing processes or equilibria. These competing processes can alter the fate of the tertiary radical in ATRP, by introducing a deactivation step, in addition to the propagation, or branch formation, available in FRP. Various simulations show that, in order to effectively decrease the branching fraction in ATRP, the tertiary radical must be deactivated relatively rapidly. Then, the rate of branch formation is slower than the rate of transfer, resulting in a decrease in the branching fraction. Kinetic simulations also find that concentrations of copper catalysts have minimal effect on the branching fractions and that higher initiator concentrations tend to decrease the branching levels in ATRP. Furthermore, Monte Carlo simulations found that chain length dependence and presence or absence of intermolecular transfer had minimal effect on the branching fraction.

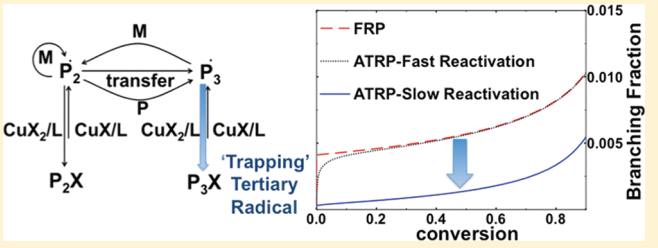

INTRODUCTION

Polymers can be branched chains, even when the linear chain architecture is targeted. These branches are generated through transfer reactions both to polymer (and also to monomer) during polymerization.[1] In polymerization of monomers such as ethylene or vinyl acetate, branching reactions have been well-studied,[1,2] and the presence of branches can have a profound impact on the properties of the resulting polymers. This is exemplified by the fact that low-density polyethylene has many branch points and a low degree of crystallinity, while high-density polyethylene has few branch points and a much higher degree of crystallinity and is a much stronger material.[3] Unlike vinyl acetate and ethylene, which have been known to undergo transfer reactions for over 50 years,[2a−c] branching in polyacrylates was discovered only in the past two decades when ^{13}C NMR studies showed quaternary branch points formed by transfer reactions.[4] Because of the influence of branches on the properties of the resulting material, it is important to accurately determine the factors, which affect the extent of branching in the macromolecules formed.

In the polymerization of acrylates, branches are typically formed by one of two processes. The first, and typically dominant, process is that of intramolecular chain transfer, i.e., backbiting.[5] In this case the secondary propagating radical abstracts a hydrogen atom from the same polymer chain, typically the pen-penultimate monomer unit behind the propagating secondary radical. The intramolecular transfer via a cyclic six-membered transition state is shown as the top reaction pathway in Scheme 1.[5] This intramolecular process gives a short chain branch after reaction of monomer with the tertiary radical. An alternative reaction pathway by which branches can be formed in acrylate systems is the intermolecular transfer shown as the lower reaction pathway in Scheme 1.[5] In this case, the secondary radical abstracts a proton from a different polymer chain, placing the tertiary radical randomly along the second polymer

Received: July 24, 2011
Revised: September 26, 2011
Published: October 13, 2011

Scheme 1. Mechanism of Short Chain Branching by Backbiting (Top Reaction Pathway) and Long Chain Branching by Intermolecular Hydrogen Abstraction (Lower Reaction Pathway) in Acrylate Polymerization[a]

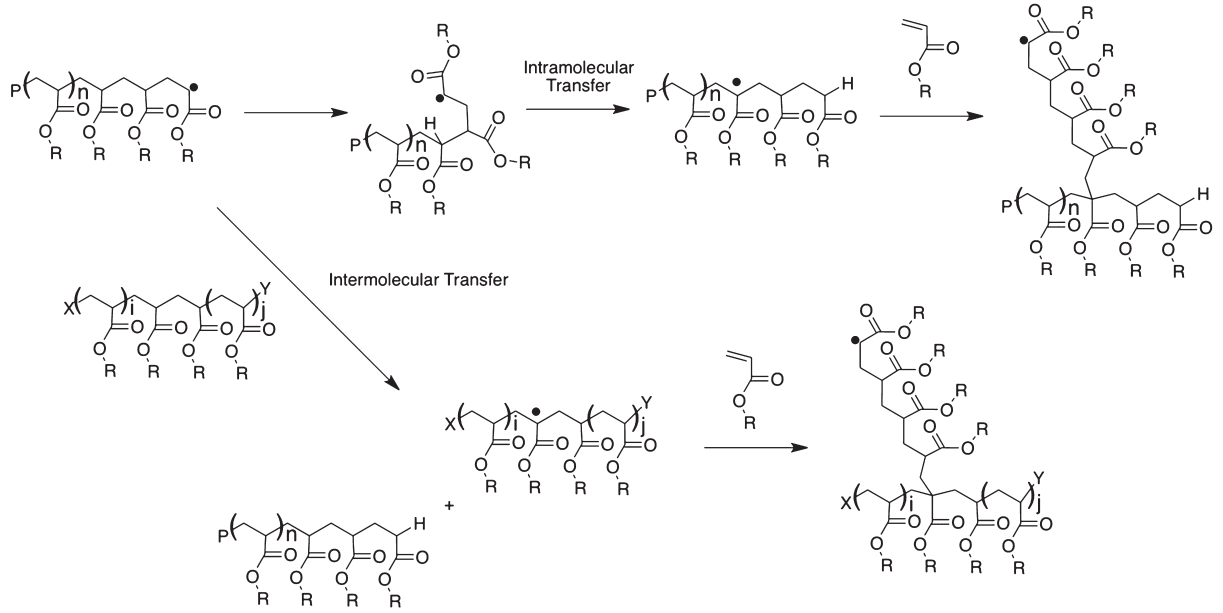

[a] Y can represent the capping agent in controlled radical polymerization, e.g., halogen in atom transfer radical polymerization (ATRP) or nitroxide in nitroxide-mediated polymerization (NMP), or an end-group in free-radical polymerization (FRP). X and P represent initiating sites or initiator fragments.

Scheme 2. Process of β-Scission in Acrylate Polymerization, Which Can Result in a Long Chain Branch, by Propagation of the Resulting Macromonomer[a]

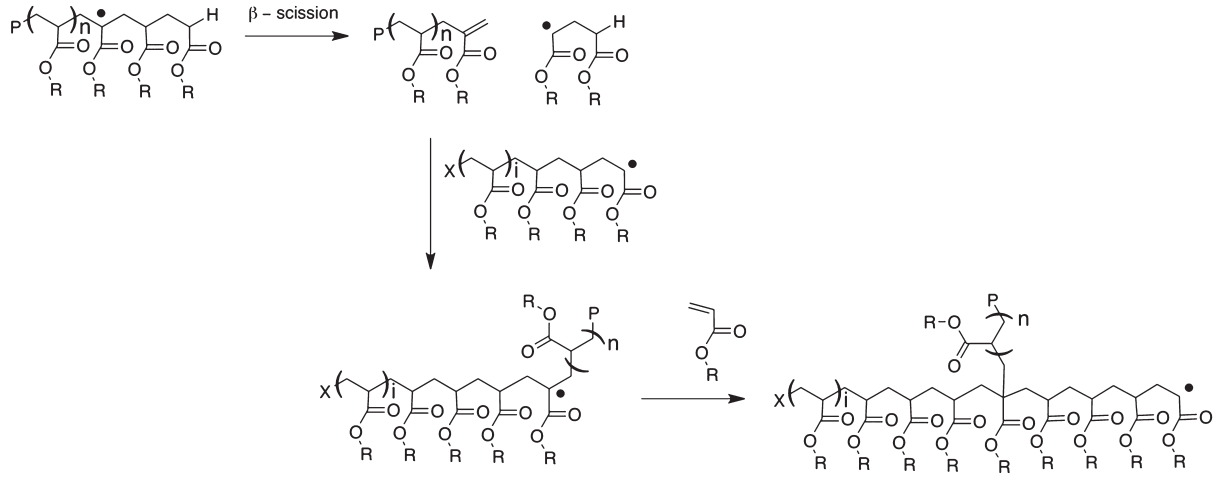

[a] X and P represent initiating sites or initiator fragments.

backbone. In general, this leads to a long chain branch after the newly formed tertiary radical propagates.[5] However, Charleux et al.[6] demonstrated using mass spectroscopy that, under typical conditions in nitroxide-mediated polymerization (NMP) of *n*-butyl acrylate, the majority of transfer reactions are due to intramolecular rather than intermolecular reactions. These results suggest that under typical conditions the majority of branches formed in an acrylate polymerization will be short chain branches rather than long chain branches. We have recently confirmed by atomic force microscopy (AFM) studies of the molecular brushes with acrylate backbone that the proportion of long chain branching is indeed very small (<0.04%) and much smaller than the overall branching estimated by ^{13}C NMR under similar conditions.[7] Interestingly, for more polar acrylates, such as 2-hydroxyethyl acrylate, there appears to be a strong dependence of the branching number on the polarity of the solvent.[8] In particular, the hydrogen bonding in 2-hydroxyethyl acrylate decreases the branching fraction significantly. The addition of a solvent that disrupts hydrogen bonds also affects the branching fraction.[8] Furthermore, the introduction of a hydrogen-bonding solvent, such as butanol, leads to a decrease of branching in poly(butyl acrylate).[8]

In addition, at sufficiently high temperatures long chain branches can be formed through β-scission of the tertiary radicals formed.[5,9] This is because one of the products of β-scission is a macromonomer, which can subsequently be incorporated into a polymer chain, leading to a long chain branch.[5] This process of long chain branching by β-scission and incorporation of the macromonomer is shown in Scheme 2.[10]

Several methods can be used to characterize the extent of branching in acrylates. One of the most common methods is ^{13}C NMR,[4a,11] with solid state NMR giving the highest resolution.[11b,e,12] The ^{13}C NMR experiment measures the total quantity of branches evaluated by the content of quaternary carbon atoms and does not distinguish between long and short chain branches.[11e,13] Alternatively, the difference in size of branched and linear macromolecules can be used to characterize the extent of primarily long chain branching polymers using techniques such as size-exclusion chromatography (SEC).[11b,d,14] Other methods include rheology[15] and direct AFM imaging of brushes based on poly(acrylate) backbones.[7] Furthermore, in recent work Klumperman et al.[16] detected the secondary and tertiary nitroxide-capped species using ^{1}H NMR.

The impact of branching can also be influenced by the pulse frequency in pulsed laser polymerization−size exclusion chromatography (PLP-SEC). At lower pulse frequencies the average degree of polymerization of the polymer is high, and the average polymer has a nontrivial number of branches, leading to contributions to the propagation by both tertiary and secondary species and a broadening of the PLP-SEC distribution. In contrast, higher pulse frequencies lead to lower average degrees of polymerization and much less impact of the branching on the PLP-SEC distribution.[17]

In recent decades the field of polymer chemistry has been revolutionized by the development of controlled/living radical polymerization (CRP) techniques.[18] These techniques include nitroxide-mediated polymerization (NMP),[19] atom transfer radical polymerization (ATRP),[20] and reversible addition−fragmentation chain transfer (RAFT) polymerization.[21] The main advantage of these CRP techniques is that they provide similar control over polymer architecture and composition as traditional ionic living polymerizations,[22] but through a radical mechanism with intermittent activation−deactivation. This allows CRP methods to be applied to a very wide range of functional groups with tolerance to impurities similar to that of a traditional free-radical polymerization (FRP), while still providing excellent control over the polymer architecture.[18b,23]

ATRP is one of the most versatile CRP methods[18b,20c,24] and uses transition metal catalysts, commonly copper-based, to activate an alkyl halide to generate a (macro)radical, which typically adds a few monomers before being deactivated by the higher oxidation state transition metal catalyst.[25] One of the most interesting experimental observations is that the fraction of branches per repeat unit in polyacrylates synthesized by CRP methods, most notably ATRP, is significantly lower than in FRP.[26] This phenomenon has been observed by both ^{13}C NMR studies[26] and more recently by directly imaging brush molecules based on acrylic backbones.[7] In addition, the reduced importance of branching in CRP has been confirmed by kinetic modeling of isobornyl acrylate polymerized under ATRP conditions.[27]

Initially, this reduced branching for typical CRPs seems counterintuitive since the radical transfer process involved in branching should be independent of whether the chain undergoes

Scheme 3. Three Interconnected and Competing Processes Involved in the ATRP of Acrylates[a]

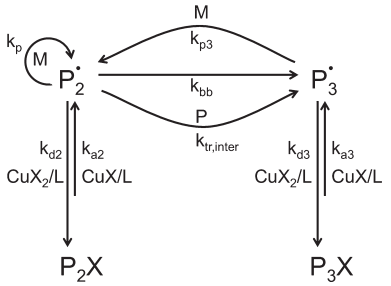

[a] The left reaction is the secondary ATRP activation−deactivation process. The right reaction is the tertiary ATRP activation−deactivation process. The top process is the nonreversible (but two-way) transformation of the secondary macroradical to the tertiary macroradical (backbiting) and of the tertiary macroradical to the secondary one (tertiary propagation); intermolecular chain transfer will be considered later, and it is only a minor contribution. Furthermore, both secondary and tertiary macroradicals undergo termination reactions; however, under typical CRP conditions these termination reactions play a minor role.

activation−deactivation processes. This is because the radical formed in CRP has the same properties as the radical formed in conventional FRP.[26,28,29] The initial hypothesis proposed to explain this phenomenon was that there is a strong chain length dependence of the transfer rate coefficients, with short chains having a higher tendency to undergo branching than long chains.[26] Since CRP reactions have predominantly long chain radicals after a very short period into the polymerization, while FRP has a continuous feeding of short radicals, this strong chain length dependence could explain the higher branching observed in FRP compared to CRP.[26] However, in subsequent work Reyes and Asua[30] simulated branching reactions both in controlled and free radical systems, finding minimal influence of chain length dependence but instead proposing that the branching was determined by the deactivation rate. Reyes and Asua[30] claimed that as long as the transient radical lifetime is lower than the average time for backbiting, the branching fraction will be lower in CRP than FRP.

In this paper it is illustrated that in ATRP (and other CRP techniques) not only the deactivation rate but several competing factors such as dynamics and thermodynamics of the equilibrium between the tertiary active and dormant species and the concentrations of various species can affect the branching. In particular, this paper will show by both a deterministic and a stochastic approach that only certain ATRP reaction systems give rise to lower branching fractions than observed for FRP. This will be justified through the concept of competitive equilibria or processes for the secondary and tertiary species. The concept of competitive equilibria in ATRP was already proposed for electron transfer reactions and reactions involving the metal complex.[31] The branching in acrylate polymerizations also resembles copolymerization of two comonomers with different ATRP equilibrium constants.[32] In such systems, the relative rates of consumption of the two comonomers (or branching in the case studied here) in FRP and ATRP become equal only after the ATRP equilibria between all active and dormant species are established, and the rates of interconversion between various active species are equal. Until this happens one monomer can be

Table 1. Reaction Scheme Used To Study Branching in the ATRP of Acrylates

$RX + CuX \xrightarrow{k_a} R^{\cdot} + CuX_2$	(1)
$R^{\cdot} + CuX_2 \xrightarrow{k_d} RX + CuX$	(2)
$R^{\cdot} + M \xrightarrow{k_p} P(1)^{\cdot}$	(3)
$P(j)^{\cdot} + M \xrightarrow{k_p} P(j+1)^{\cdot}$	(4)
$P(j)^{\cdot} + CuX_2 \xrightarrow{k_d} P(j)X + CuX$	(5)
$P(j)X + CuX \xrightarrow{k_a} P(j)^{\cdot} + CuX_2$	(6)
$P(j)^{\cdot} \xrightarrow{k_{bb}} P_3(j)^{\cdot}$	(7)
$P_3(j)^{\cdot} + CuX_2 \xrightarrow{k_{d3}} P_3(j)X + CuX$	(8)
$P_3(j)X + CuX \xrightarrow{k_{a3}} P_3(j)^{\cdot} + CuX_2$	(9)
$P_3(j)^{\cdot} + M \xrightarrow{k_{p3}} P(j+1)^{\cdot}$	(10)
$R^{\cdot} + R^{\cdot} \xrightarrow{k_{t0}} D$	(11)
$P(j)^{\cdot} + R^{\cdot} \xrightarrow{k_{t0}} D(j)$	(12)
$P(j)^{\cdot} + P(k)^{\cdot} \xrightarrow{k_t} D(j+k)$	(13)
$P_3(k)^{\cdot} + R^{\cdot} \xrightarrow{k_{t0}} D(j)$	(14)
$P(j)^{\cdot} + P_3(k)^{\cdot} \xrightarrow{k_t} D(j+k)$	(15)
$P_3(j)^{\cdot} + P_3(k)^{\cdot} \xrightarrow{k_t} D(j+k)$	(16)

consumed faster than the other one. This work will show that a similar concept holds for branching in acrylate polymerizations, where the presence of competing processes can lead to an imbalance of the rates of interconversion between secondary and tertiary species, which in turn results in a branching rate significantly lower than that seen in FRP under typical ATRP conditions.

RESULTS AND DISCUSSION

Competitive Processes in ATRP of Acrylates. This section describes the ATRP of acrylates in light of three competitive processes. However, the concepts developed in this paper can subsequently be extended to other CRP systems such as RAFT polymerization and NMP. The three inter-related processes relevant to branching in acrylate polymerizations are shown in Scheme 3 and consist of the secondary ATRP activation−deactivation process (left), the tertiary ATRP activation−deactivation process (right), the transformation of secondary radicals to tertiary radicals by transfer (backbiting), and the regeneration of the secondary species by addition of monomer to tertiary radicals (tertiary propagation).

These three processes can be characterized by different rates, and the rate of one reaction can influence the rates of the other reactions. It will be shown in this paper that the three processes shown in Scheme 3 are needed to explain the reduction of branches observed in acrylates polymerized by ATRP as compared to FRP. It will be shown that these three processes compete with each other and force for instance one, or even two, of these processes to be out of balance for much of the reaction process. Note that this competitive interaction is a feature of CRP of acrylates, since the FRP process only has the transfer and tertiary propagation steps. This implies that only this reaction needs to be balanced in FRP, which typically occurs very rapidly. It will be shown that the order in which these reaction rates balance in the CRP of acrylates will depend on the rate coefficients. Furthermore, it will be demonstrated that different reaction conditions, such as the ATRP initial initiator concentration, can influence the rate at which these three processes reach a balanced state.

PREDICI and Kinetic Monte Carlo Simulations of Branching in Acrylate Polymerization. Two different mathematical techniques are used to characterize the extent of branching in acrylate polymerizations. The first technique is based upon the integration of rate equations using the PREDICI software package. The second technique is based on kinetic Monte Carlo (kMC) methods and uses stochastic methods to predict branching. These two techniques are complementary to each other, with the PREDICI simulations being simple to implement and computationally inexpensive, while the kMC simulations allow greater flexibility and the monitoring of individual polymers. In particular, it will be shown that these two techniques are in excellent agreement when simulating the same system.

PREDICI Simulations. The reaction scheme in Table 1 was implemented in PREDICI (v 6.3.2) to study the branching in the ATRP of acrylates. Intermolecular transfer reactions were neglected at that stage based on literature data.[6,7]

Similarly, PREDICI simulations of the FRP of acrylates were performed based on the reactions listed in Table 2. This kinetic scheme has the same propagation, backbiting, and termination reaction as before, except that the radical source is now a conventional initiator R_2 and there are no ATRP activation−deactivation processes, due to the absence of the copper catalyst.

The instantaneous branching fraction $f_{br,i}$ was calculated as the ratio of number of tertiary propagations to the total number of propagations. However, because of the much lower rate of tertiary versus secondary propagation, the total number of propagations can be well approximated as only the number of secondary propagations. Therefore, the instantaneous branching fraction is calculated by

$$f_{br,i} = \frac{k_{p3}[P_3^{\bullet}]}{k_p[P^{\bullet}]} \quad (28)$$

By determining the total concentration of branch points, [B], as the integral of $k_{p3}[M][P_3^{\bullet}]$ over the reaction time, the cumulative branching fraction $f_{br,c}$ can be obtained as

$$f_{br,c} = \frac{[B]}{[M]_0 - [M]} \quad (29)$$

where $[M]_0$ is the initial monomer concentration and [M] is the monomer concentration at the point of interest.

The rate coefficients used in the simulations are given in Table 3, with only the parameters k_{a3} and k_{d3} being varied. The rate coefficients are chosen to mimic the polymerization of

Table 2. Reaction Scheme To Study Branching in the FRP of Acrylates

$R_2 \xrightarrow{k_i} 2\,R^{\cdot}$	(17)
$R^{\cdot} + R^{\cdot} \xrightarrow{k_{t0}} D$	(18)
$R^{\cdot} + M \xrightarrow{k_p} P(1)^{\cdot}$	(19)
$P(j)^{\cdot} + M \xrightarrow{k_p} P(j+1)^{\cdot}$	(20)
$P(j)^{\cdot} \xrightarrow{k_{bb}} P_3(j)^{\cdot}$	(21)
$P_3(j)^{\cdot} + M \xrightarrow{k_{p3}} P(j+1)^{\cdot}$	(22)
$P(j)^{\cdot} + R^{\cdot} \xrightarrow{k_{t0}} D(j)$	(23)
$P(j)^{\cdot} + P(k)^{\cdot} \xrightarrow{k_t} D(j+k)$	(24)
$P_3(k)^{\cdot} + R^{\cdot} \xrightarrow{k_{t0}} D(j)$	(25)
$P(j)^{\cdot} + P_3(k)^{\cdot} \xrightarrow{k_t} D(j+k)$	(26)
$P_3(j)^{\cdot} + P_3(k)^{\cdot} \xrightarrow{k_t} D(j+k)$	(27)

n-butyl acrylate at 70 °C, with as many rate coefficients chosen to match those used by Reyes and Asua in their recent kinetic Monte Carlo simulations.[30]

For secondary ATRP (de)activation, representative rate coefficients are used based on the work of Tang et al.[33] This study reports deactivation rate coefficients for acrylic like secondary radicals to secondary alkyl bromides at 22 °C in the order of 10^7-10^8 M^{-1} s^{-1}. In this paper, the upper limit of 1×10^8 M^{-1} s^{-1} was chosen taking also into account the higher temperature considered. Analogously for activation of secondary alkyl bromides, Tang et al.[33] reported values in the range of $10^{-2}-10^1$ M^{-1} s^{-1} at 22 °C. In agreement with the known influence of temperature[34] on this coefficient, a value of 10^0 M^{-1} s^{-1} was selected.

On the other hand, the corresponding tertiary rate coefficients k_{d3} and k_{a3} were systematically varied in the range $k_{d3} = 10^4-10^8$ M^{-1} s^{-1} and $k_{a3} = 10^{-3}-10^3$ M^{-1} s^{-1} with the values $k_{d3} = 10^7$ M^{-1} s^{-1} and $k_{a3} = 10^0$ M^{-1} s^{-1} as reference values. Note that these values give a 1 order of magnitude higher equilibrium constant for the tertiary radicals than for the secondary radicals. The tertiary deactivation rate coefficient was selected to be 10 times smaller than the secondary one due to both higher radical stability and steric effects. The activation rate coefficient was not increased due to expected steric effects requiring a catalyst to approach congested alkyl halide for the concerted inner-sphere electron-transfer process. However, both values were varied systematically.

The termination rate coefficients were chosen to qualitatively match the trends seen using chain-length-dependent (apparent) termination rate coefficients.[27,35,36] In particular, the unimeric termination rate coefficient was chosen to be 10^9 M^{-1} s^{-1}, in agreement with the rate coefficients observed experimentally for small chains.[37] The macroradical termination rate coefficient was taken to be 10^8 M^{-1} s^{-1}, with no chain length dependence.

Table 3. Kinetic Coefficients Used in PREDICI Simulations of the FRP and ATRP of *n*-Butyl Acrylate at 70 °C[a]

rate coefficient	value	reference
k_a	1×10^0 M^{-1} s^{-1}	this work
k_d	1×10^8 M^{-1} s^{-1}	this work
k_p	41400 M^{-1} s^{-1}	17a, 30
k_{bb}	1200 s^{-1}	30, 41
k_{p3}	153 M^{-1} s^{-1}	30, 42
k_i	3.2×10^{-5} M^{-1} s^{-1}	39
k_{t0}	1×10^9 M^{-1} s^{-1}	35a, 35b
k_t	1×10^8 M^{-1} s^{-1}	35a, 35b

[a] For the ATRP case, tertiary activation/deactivation rate coefficients varied in the range $10^{-3}-10^3$ M^{-1} s^{-1}/10^4-10^8 M^{-1} s^{-1}.

Although there is in general chain length dependence of the termination rate coefficient, in this illustrative work on branching in acrylates an average k_t of 10^8 M^{-1} s^{-1} was assumed, consistent with the typical termination rate coefficients observed for acrylic macroradicals.[35b,38]

Finally, for the free radical initiator dissociation coefficient, the value typical for azo bis(isobutyronitrile) (AIBN) at 70 °C is used.[39] Although initiator efficiencies have not been explicitly accounted for in this model,[40] the inclusion will only change the evolution of conversion with time, rather than change the evolution of branching fraction with conversion, which is the quantity that is of interest in this work.

Reaction Rates and Branching Fraction in Bulk FRP. Figure 1 left shows the rate of secondary and tertiary propagation and backbiting in a bulk polymerization with $[M]_0:[R_2]_0$ = 7000:1. Clearly, the FRP system quickly (within 200 ms) reaches a balance between the rates of backbiting and tertiary propagation; i.e., the quasi-steady-state approximation for the tertiary radical species is valid. Figure 1, right, clearly shows that for the FRP case such balance leads to a high cumulative branching fraction from low conversion onward.

Reaction Rates and Branching Fraction in ATRP. The first effect studied in the ATRP of acrylates was the effect of the tertiary ATRP dynamics on the rates of secondary propagation, backbiting, tertiary propagation, secondary and tertiary activation, and deactivation with the fixed tertiary ATRP equilibrium constant and targeting a chain length of 200. In a next step the effect of the equilibrium constant on these rates for a fixed deactivation rate coefficient was investigated. Finally, a more detailed study was performed as a function of reaction conditions. In all cases, a comparison is made with the FRP case discussed above.

1. Importance of the ATRP Dynamics for a Fixed Equilibrium Constant. Figure 2 shows the rate data for two extreme cases with the tertiary ATRP equilibrium constant the same and equal to 10^{-7}, i.e., 10 times higher than for the secondary species (reference value; see above). The left subfigure corresponds to the case assuming a tertiary radical deactivation rate coefficient of $k_{d3} = 10^7$ M^{-1} s^{-1}, whereas the right subfigure corresponds to a slower tertiary radical deactivation ($k_{d3} = 10^4$ M^{-1} s^{-1}). Clearly, the secondary rates of propagation, ATRP activation, and ATRP deactivation are essentially unchanged by the dynamics of tertiary species, with the secondary radical reaching ATRP equilibrium very rapidly (~5% conversion). Note that in both cases the rates of backbiting are close to 0.5×10^{-5} M^{-1} s^{-1} for the majority of the polymerization. However, as expected, there

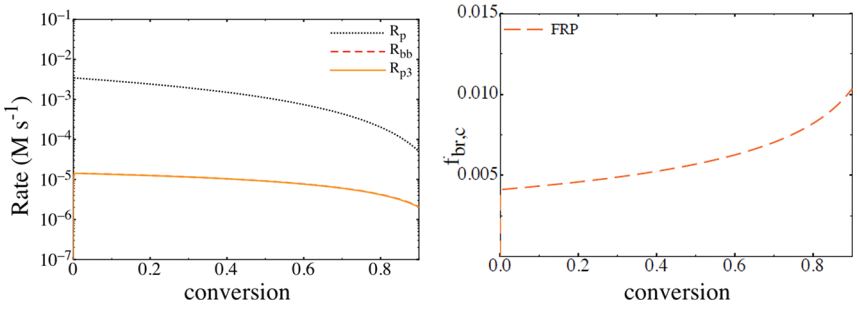

Figure 1. Rate data (left) and cumulative branching fraction (right) for bulk FRP of *n*-butyl acrylate under the conditions $[M]_0:[R_2]_0 = 7000:1$. Rates of secondary propagation (R_p), backbiting (R_{bb}), and tertiary propagation or branching (R_{p3}) are shown, with the rate of tertiary propagation matching the rate of backbiting for the whole reaction.

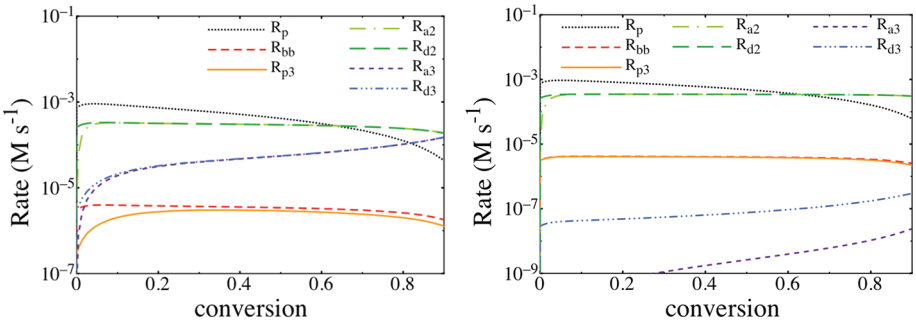

Figure 2. Rate data for bulk ATRP of *n*-butyl acrylate under the conditions $[M]_0:[RX]_0:[CuX]_0:[CuX_2]_0 = 200:1:0.29:0.029$. Both have tertiary species equilibrium constants of 10^{-7} (reference value). The left has a tertiary radical deactivation rate coefficient 10^7 M^{-1} s^{-1}; the right has a tertiary radical deactivation rate coefficient of 10^4 M^{-1} s^{-1}. These data show the rates of secondary radical propagation (R_p), backbiting (R_{bb}), tertiary radical propagation or branching (R_{p3}), secondary species ATRP activation (R_{a2}), secondary radical ATRP deactivation (R_{d2}), tertiary species ATRP activation (R_{a3}), and tertiary radical ATRP deactivation (R_{d3}).

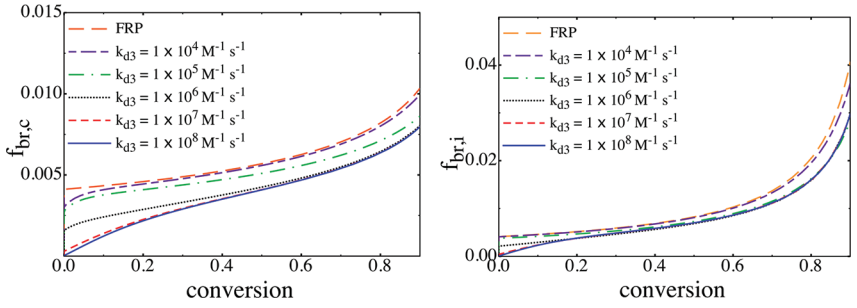

Figure 3. Branch fraction data for bulk ATRP of *n*-butyl acrylate under the conditions $[M]_0:[RX]_0:[CuX]_0:[CuX_2]_0 = 200:1:0.29:0.029$. All systems have tertiary ATRP equilibrium constants of 10^{-77} (reference value). Left shows cumulative branching fraction, right shows instantaneous branching fraction data.

is a significant influence of the tertiary radical activation—deactivation reaction dynamics on the fate of tertiary radicals and interestingly on the order of reaching the equilibrium. When the tertiary radical system has fast ATRP dynamics, the tertiary species reach ATRP equilibrium at low conversion (~10%). The order in which the reaction rates match is: secondary ATRP equilibrium first followed by the tertiary ATRP equilibrium with no balance in the rates of tertiary—secondary exchange; during the whole ATRP the rate of tertiary propagation is below the rate of backbiting. Hence, for fast ATRP dynamics, the inter-relation of the ATRP rates strongly differs from the FRP case, indicative of different branching fractions (cf. Figure 3). In contrast when the ATRP dynamics of the tertiary radicals are slow, the rate of tertiary radical propagation equals to that of backbiting for essentially the whole reaction, as for the FRP case (resulting in similar branching as in FRP; cf. Figure 3); the rate of tertiary radical deactivation is very low, and there is virtually no tertiary species activation. In this case, the tertiary—secondary interchange balances first, as seen by agreement between the rate of tertiary propagation and backbiting, followed by the secondary species ATRP equilibrium, with the tertiary species ATRP never reaching equilibrium.

The discussed rate data are reflected in both the cumulative and instantaneous branching fractions shown in Figure 3. When the ATRP dynamics for tertiary species are fast, the instantaneous and cumulative branching fractions are well below the FRP

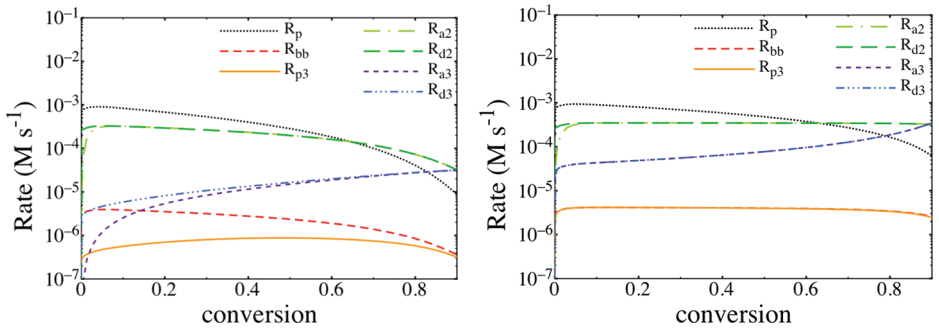

Figure 4. Rate data for bulk ATRP of *n*-butyl acrylate under the conditions $[M]_0:[RX]_0:[CuX]_0:[CuX_2]_0 = 200:1:0.29:0.029$. Both have tertiary radical deactivation rate coefficients of 10^7 M^{-1} s^{-1}. The left has equilibrium constant 10^{-8} the right has equilibrium constant 10^{-5}. These data show the rates of secondary radical propagation (R_p), backbiting (R_{bb}), tertiary radical propagation or branching (R_{p3}), secondary ATRP species activation (R_{a2}), secondary radical deactivation (R_{d2}), tertiary species ATRP activation (R_{a3}), and tertiary radical deactivation (R_{d3}).

limit, whereas the FRP limit is reached for the opposite case. These results are consistent with the results of Reyes and Asua, who also found that short transient radical lifetimes are needed for the branching fraction in CRP to be lower than in FRP.[30] The reason for this observation is that a system with rapid deactivation of the tertiary radical can efficiently form the halogen-capped dormant tertiary species. In contrast, when the tertiary deactivation rate is low, the monomer adds to the mid-chain radical before the CuX_2 can deactivate the chain. One important observation is that regardless of the fate of the tertiary radical, deactivation or propagation, the control over the properties of the polymers for the studied catalyst reactivities remains good. This can be seen in the Supporting Information (Figure S1) which plots both the evolution of number-average degree of polymerization (DP_n) and M_w/M_n values with conversion for the case of low branching ($k_{d3} = 10^7$ M^{-1} s^{-1}) and high branching ($k_{d3} = 10^4$ M^{-1} s^{-1}). In both cases the number-average degree of polymerization closely adheres to theory since the target DP was 200 and the molecular weight distribution was narrow.

However, as will be shown further, other factors also influence the branching fractions in ATRP. Importantly, in this discussion it is illustrated that whenever the rate of backbiting matches the rate of tertiary propagation, the instantaneous branching fraction matches the FRP limit.

2. Importance of the ATRP Equilibrium Constant at a Fixed Deactivation Rate Coefficient. The second effect studied in the ATRP case was the effect of the equilibrium constant for tertiary species on the rates and branching fractions. In all cases the tertiary radical deactivation rate coefficient was 10^7 M^{-1} s^{-1}, and the tertiary species activation rate coefficients were varied between 10^{-1} and 10^2 M^{-1} s^{-1}. Figure 4 shows the effect of the tertiary species equilibrium constant on the rates of propagation, backbiting, and ATRP activation and deactivation. These data show that the rate of secondary radical propagation and secondary species activation and deactivation are not changed significantly. However, the tertiary species ATRP rates and the rate of tertiary radical propagation are significantly influenced by the tertiary species ATRP equilibrium constant. In this case, a high tertiary species ATRP equilibrium constant causes a very active tertiary radical, and almost instantaneous equilibration of the tertiary species ATRP system, and also balances the rates of backbiting and tertiary propagation. Interestingly, the rates of the three competitive processes are balanced at ~5% conversion.

Alternatively, a low tertiary species equilibrium constant drastically changes the order of rate balancing. For such a case, the secondary species ATRP equilibrium is rapidly reached, with the tertiary ATRP equilibrium reached at ~25% conversion, while a balance in the secondary/tertiary propagating species interconversion is not reached until very high conversion.

As can be seen in Figure 5, the systems with high equilibrium constant have cumulative (left) and instantaneous (right) branching fractions similar to those of FRP, while those with lower equilibrium constants have values far below that of FRP. This is due to the fact that a sufficiently high tertiary species equilibrium constant increases concentration of the radical, while the low equilibrium constant favors the dormant form. When the dormant form is favored, the branching fraction is reduced since the radicals formed by backbiting are essentially trapped in the dormant form. In contrast, a more active system leads to a higher branching fraction due to the higher concentration of tertiary radicals which can reform the secondary species by branching reactions. One interesting feature seen in the $K_{ATRP,3} = 10^{-8}$ profile (Figure 5 right) is that the instantaneous branching fraction approaches that of the FRP limit, at the same point where the backbiting rate converges to the tertiary propagation rate (Figure 4, left). However, this occurs only at high conversion, and consequently the cumulative (experimentally measurable) branching fraction is far below the FRP limit. In contrast, the instantaneous and cumulative branching profiles for the $K_{ATRP,3} = 10^{-5}$ case in Figure 5 show close agreement between the FRP limit and the ATRP data due to the high ATRP equilibrium constant. This is consistent with the rate data in Figure 4, right, which shows good agreement between the rate of backbiting and the rate of tertiary propagation throughout the ATRP.

Hence, even for a constant tertiary deactivation rate coefficient, it is possible to have either a significant decrease in the cumulative branching fraction, as compared to the FRP case, as in the $K_{ATRP,3} = 10^{-8}$ case or, alternatively, a very small decrease, as in the $K_{ATRP,3} = 10^{-5}$ case. Clearly, an explanation solely based on a difference in deactivation rate and, hence radical lifetime,[30] is not sufficient to explain the difference in branching fractions in ATRP and FRP. Instead, the consideration of competing processes or reaction pathways is necessary.

3. Importance of Reaction Conditions. In this section the effect of reaction conditions, such as the initial concentration of the (de)activator and the initiator and the presence of solvent, on the reaction rates and cumulative branching fraction is presented. In all simulations, the reference values for K_{ATRP-3} and k_{d3} are used (K_{ATRP-3} 10^{-7} and $k_{d3} = 10^7$ M^{-1} s^{-1}). From the kinetic point of view the effect of changing concentrations of Cu

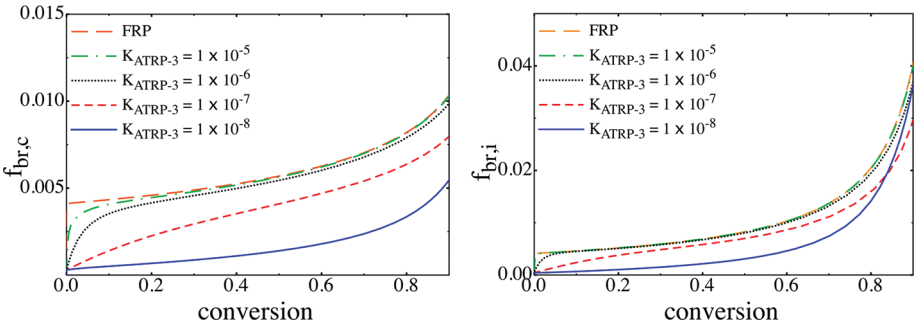

Figure 5. Branch fraction data for bulk ATRP of *n*-butyl acrylate under the conditions $[M]_0:[RX]_0:[CuX]_0:[CuX_2]_0$ = 200:1:0.29:0.029. All systems have tertiary deactivation rate coefficients of 10^7 M^{-1} s^{-1}. The left shows cumulative branching fraction, and the right shows instantaneous branching fraction data.

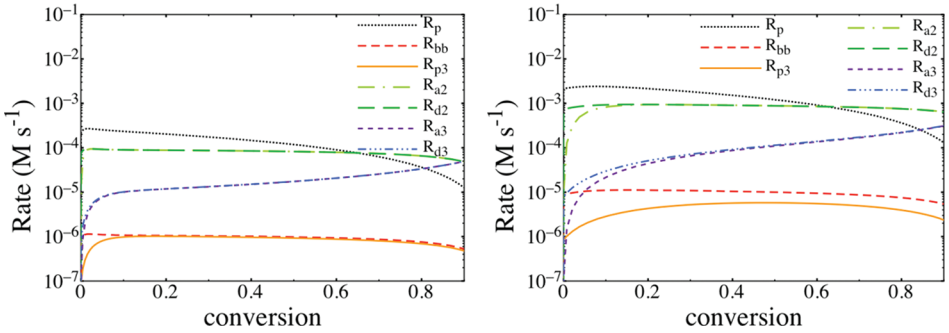

Figure 6. Rate data for bulk ATRP of *n*-butyl acrylate under the conditions $[M]_0:[RX]_0:[CuX]_0:[CuX_2]_0$ = 200:0.29:0.29:0.029 (left) and $[M]_0:[RX]_0:[CuX]_0:[CuX_2]_0$ = 200:2.9:0.29:0.029 (right). Both have tertiary species equilibrium constants of 10^{-7}, and deactivation rate coefficients of 10^7 M^{-1} s^{-1} (reference values). These data show the rates of secondary radical propagation (R_p), backbiting (R_{bb}), tertiary radical propagation or branching (R_{p3}), secondary species ATRP activation (R_{a2}), secondary radical deactivation (R_{d2}), tertiary species ATRP activation (R_{a3}), and tertiary radical deactivation (R_{d3}).

compounds is similar to the effect of changing the activation (Cu^I) or deactivation (Cu^{II}) rate coefficients by the same factor for secondary and tertiary species.

The Supporting Information shows the rate and branching fraction data in cases where the concentrations of the CuX activator and CuX_2 deactivator were varied. In particular, the rate and branching fraction data shown in the Supporting Information show that the concentration of the CuX activator has essentially no effect on the branching fraction. This is because increasing the concentration of the CuX activator by a given factor increases all reaction rates by a same relative factor, implying no net change in the branching fraction with conversion (Figures S2 and S3).

Similarly, the effect of the CuX_2 deactivator is quite minor, as long as there is a sufficient amount of CuX_2 to efficiently deactivate the tertiary radical. When there is no added CuX_2, the rates of secondary and tertiary propagation are very high initially (Figure S4), and in this early phase the branching fraction is close to the FRP limit (Figure S5). However, after this initial phase there is a sufficient amount of CuX_2 generated by radical terminations, and the branching fraction approaches the value observed in systems where there is a nontrivial amount of CuX_2 added (Figure S5). Moreover, above a certain minimal concentration of CuX_2, further additions of CuX_2 lead to no change in the branching fraction with conversion, since higher CuX_2 concentrations slow down all rates by the same relative factor.

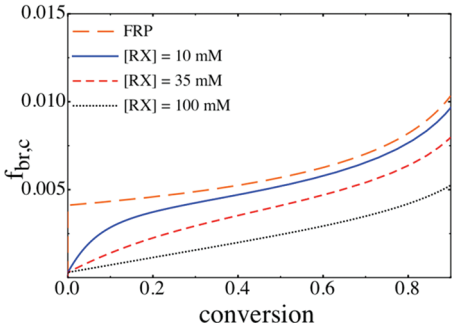

Figure 7. Cumulative branch fraction data for bulk ATRP of *n*-butyl acrylate under conditions $[M]_0:[CuX]_0:[CuX_2]_0$ = 200:0.29:0.029. All have tertiary equilibrium constants of 10^{-7} and deactivation rate coefficients of 10^7 M^{-1} s^{-1} (reference values). $[M]_0:[RX]_0$ was varied from 200:0.29 to 200:2.9.

The next parameter investigated was the concentration of the ATRP initiator, which changed the targeted degree of polymerization (DP). As can be seen in Figure 6, increasing the initiator concentration (i.e., lowering the targeted DP) increases all rates; however, the secondary propagation rate increases linearly with initiator concentration, as does the backbiting rate, whereas the tertiary radical propagation rate only increases by approximately a factor of 3. For this reaction conditions, the order of reaction balancing is secondary ATRP equilibrium first, then tertiary

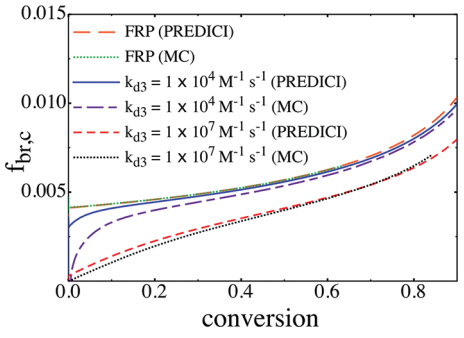

Figure 8. Comparison of simulated cumulative braching fractionin bulk FRP and ATRP using PREDICI and kMC. FRP: $[M]_0$= 6.97 M and $[R_2]_0$ = 1 mM; for ATRP: $[M]_0$= 6.97 M, $[RX]_0$ = 0.0349 M, $[CuX]_0$ = 10 mM, $[CuX_2]_0$ = 1 mM, $k_p = 4.14 \times 10^4$, $k_{p3} = 153$, $k_t = 1 \times 10^8$, $k_d = 1 \times 10^8$, $k_a = 1$, $k_{d3} = 10^7$ or 10^4, $k_{a3} = 1$ or 10^{-3} (the tertiary ATRP equilibrium constant was 10^{-7}; reference values), all in M^{-1} s^{-1}, and $k_{bb} = 1.2 \times 10^3$ s^{-1}.

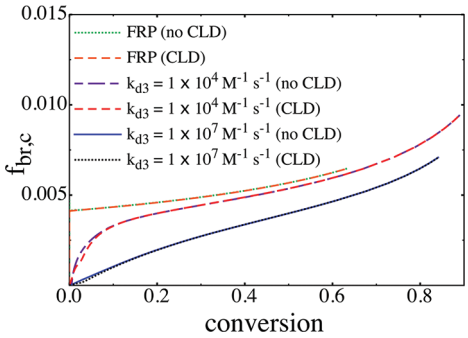

Figure 9. Comparison of simulated cumulative branching fraction in FRP and ATRP with and without chain-length dependency (CLD) of rate coefficients, using kMC simulations. FRP: $[M]_0$= 6.97 M and $[R_2]_0$ = 1 mM; $[M]_0$ = 6.97 M, $[RX]_0$ = 0.0349 M, $[CuX]_0$ = 10 mM, $[CuX_2]_0$ = 1 mM, $k_p = 4.14 \times 10^4$, $k_{p3} = 153$, $k_t = 1 \times 10^8$, $k_d = 1 \times 10^8$, $k_a = 1$, k_{d3} = 10^7 or 10^4, $k_{a3} = 1$ or 10^{-3} (the equilibrium constant of tertiary activation equal to 10^{-7}; reference values), all in M^{-1} s^{-1}, and $k_{bb} = 1.2 \times 10^3$ s^{-1}. CLD according to Heuts and Russell form $k(i) = k(\text{long}) \times (1 + 20.4 \times \exp[-\ln(2) \times (i - 1)/0.33])$[45] was applied to all second-order rate coefficients except termination. Only backbiting three units back in the chain are taken into account in simulations.

ATRP equilibrium, and possibly branching/backbiting, although a true balance is not fully reached for the high DP case and very much not reached for the low DP case.

These rate data are corroborated by the cumulative branching fraction data in Figure 7. This plot clearly shows that lower targeted DPs lead to significantly lower branching fractions. This is an initially unexpected result, since upon first inspection the effect of the initiator should be similar to the effect of the CuX activator, since both increase the polymerization rate. However, the higher initiator concentration also leads to a larger discrepancy between the concentrations of tertiary and secondary radicals at a given conversion as outlined in the Supporting Information, and also subsequently in the text, where the total number of dormant and branch species is calculated analytically as a function of conversion.

The final effect investigated was solvent dilution (cf. Figure S6). One simulation was performed in bulk and the other with exactly the same reagent molar ratios, except for 50 vol % solvent. For comparison, the similar was done for the FRP case. In particular, the rate data show that the shape of all rate curves is similar for both the concentrated and dilute case. However, the unimolecular backbiting process decreases by a smaller amount upon dilution than the other bimolecular processes, strongly indicating an increased importance of branching upon dilution, as confirmed in Figure S7.

Kinetic Monte Carlo Simulations. Kinetic Monte Carlo (kMC) methods can be used to model radical polymerizations consisting of several reactions, such as propagation, activation deactivation, backbiting, and intermolecular transfer reactions. The kMC method used in this work has been previously described,[43] and it is an alternative to the widely used Gillespie's method.[44] This method divides the reaction time into a large number of small intervals, for which it can be assumed that concentrations of all reagents are approximately constant, and stochastic operations on all reacting entities can be performed, treating the rate coefficients as "microscopic" (hypothetical) rate constants.

These kMC simulations allow a different and complementary technique to the PREDICI simulations. The kMC simulations allow a confirmation of the validity of the conclusion drawn from the PREDICI simulations, and also since kMC can be used to follow individual chains, these simulations can give insights into the characteristics of individual polymer chains, rather than the properties of the average polymer.

Comparison of PREDICI and kMC Simulations. Figure 8 compares the simulated cumulative branching fractions as obtained by kMC with those using PREDICI for the FRP case (Figure 1) and two ATRP cases, which differ in the deactivation rate coefficient selected ($k_{d3} = 10^4$ M^{-1} s^{-1} vs 10^7 M^{-1} s^{-1}; Figure 3). For this comparison, the rate coefficients listed in Table 3 were used; no chain length dependence (CLD) of the rate coefficients was considered, and intermolecular transfer reactions were neglected. Importantly, in the kMC simulations backbiting of species having a chain length of 1 and 2, which is experimentally very unlikely, was omitted, contrary to the PREDICI simulations.

Clearly, FRP plots of kMC and PREDICI simulations agree very well, since very short chains (DP < 3) contribute very little to the total macroradical population in a FRP process, in which higher DPs are already obtained from low conversions onward. Also, a good agreement for both approaches is obtained for the ATRP cases, although at low conversions some deviations can be observed. At such conversions the contribution of the very short chains (DP < 3) cannot be neglected, and hence, it follows that the performed PREDICI simulations slightly overestimate the cumulative branching fractions. However, the latter effect is leveled out at higher conversions, and it can be concluded that the kMC simulations confirm well the results obtained using PREDICI.

General Importance of Chain-Length Dependence of Rate Coefficients. Reyes and Asua[30] reported that effect of the CLD of transfer rate coefficients in FRP and CRP effects can be neglected. In this section, kMC was used to study the possible CLD of other reactions to further understand acrylate polymerizations. For the sake of simplicity, in these kMC simulations intermolecular transfer reactions were neglected.

The effect of chain length dependency on bimolecular rate coefficients, such as propagation and deactivation, etc., was investigated while keeping the same backbiting rate coefficient. Termination was not considered, however, in a well-controlled

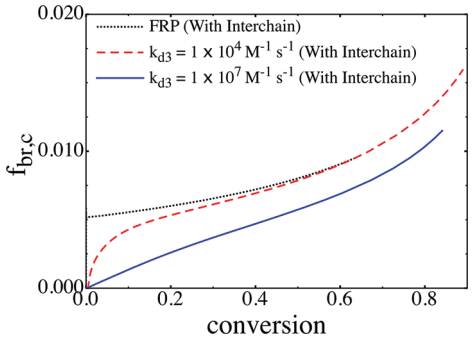

Figure 10. Cumulative branching fractions which includes the contribution of conventional backbiting, longer distance−backbiting and intermolecular transfer using kMC simulations; FRP $[M]_0 = 6.97$ M and $[R_2]_0 = 1$ mM; ATRP:$[M]_0 = 6.97$ M, $[RX]_0 = 0.0349$ M, $[CuX]_0 = 10$ mM, $[CuX_2]_0 = 1$ mM, $k_p = 4.14 \times 10^4$, $k_{p3} = 153$, $k_{tr,intert} = 133$, $k_t = 1 \times 10^8$, $k_d = 1 \times 10^8$, $k_a = 1$, $k_{d3} = 10^7$ or 10^4, $k_{a3} = 1$ or 10^{-3} (the equilibrium constant of tertiary activation equal to 10^{-7}; reference values), all in M^{-1} s^{-1}, and $k_{bb} = 1.2 \times 10^3$ s^{-1}. FRP case: termination by disproportionation (simplification not affecting the cumulative branching).

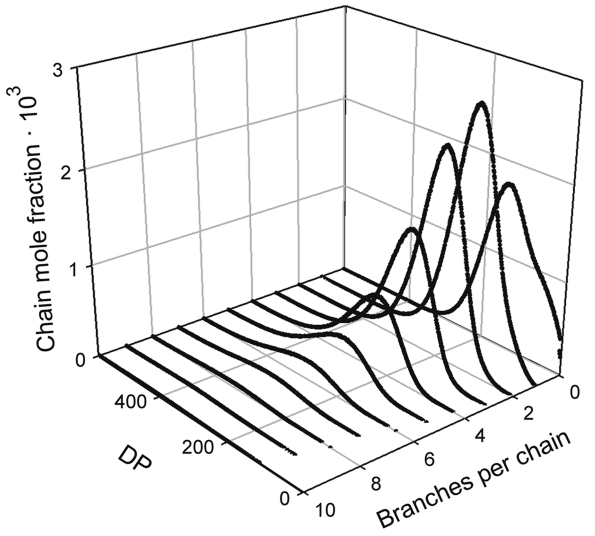

Figure 11. Distribution of polymer chains as a function of the number of branches and DP of polymer chains, computed at 92% of monomer conversion in ATRP. $[M]_0 = 6.97$ M, $[RX]_0 = 0.0349$ M, $[CuX]_0 = 10$ mM, $[CuX_2]_0 = 1$ mM, $k_p = 4.14 \times 10^4$, $k_{p3} = 153$, $k_{tr,intert} = 133$, $k_t = 1 \times 10^8$, $k_d = 1 \times 10^8$, $k_a = 1$, $k_{d3} = 10^7$ or 10^4, $k_{a3} = 1$ or 10^{-3} (the equilibrium constant of tertiary activation equal to 10^{-7}; reference values), all in M^{-1} s^{-1}, and $k_{bb} = 1.2 \times 10^3$ s^{-1}. These polymer include branching via intermolecular transfer, backbiting via rings larger than the typical six-membered one and CLD.

ATRP the influence of termination is minimal. All bimolecular rate coefficients were assumed to follow the Heuts−Russell form: $k(i) = k(\text{long}) \times (1 + 20.4 \times \exp[-\ln(2) \times (i - 1)/0.33])$.[45]

As seen in Figure 9, CLD of the rate coefficients for bimolecular reactions such as propagation, activation, deactivation, etc., has a minimal effect on the cumulative branching fraction. Note that for the ATRP case rapid deactivation of the tertiary radical and slow deactivation of the tertiary radical ($k_d = 10^4$ M^{-1} s^{-1} vs 10^7 M^{-1} s^{-1}; Figure 3) were considered. Some small differences were, however, observed for very short chains, which can be attributed to differences in rates of attaining the steady-state conditions for secondary and tertiary radicals.

When combining the conclusions derived from Figure 9 with the simulation data of Reyes and Asua,[30] the data clearly suggest that CLD of rate coefficients has minimal impact on the observed branching fractions. Hence, these results do not support the original proposition by Ahmad et al.,[26] that CLD is significant enough to alter the branching fractions observed in CRP and FRP. Further the effect of secondary dynamics is also investigated (cf. Figure S8) and shows that there is almost no effect of secondary dynamics, or absolute value of the rate coefficients, on the branching fraction.

Effect of Intermolecular Chain Transfer for Branching. The kMC simulations were also used to determine the influence of intermolecular chain transfer operating besides backbiting. As in the case of pure backbiting, the branching in ATRP was usually lower than in FRP. Intermolecular transfer can lead to macromolecules with multiple propagating sites, which can greatly affect the properties of the macromolecules, since the eventual products will be a T-shaped or three-armed stars. In addition to intermolecular transfer, the possibility of backbiting through a larger than 6-membered ring was investigated. As there are no precise experimental measurements or rate coefficient values for such larger distance intramolecular transfers available, the transfer to the fourth unit was assumed to be 10 times slower than to the third one and rate coefficients for transfers to the units located in larger distance ($x > 4$) from the secondary radical decrease were calculated according to a Jacobson−Stockmayer relationship:[46]

$$k_{bb}(x) = k_{bb}(4)(x/4)^{-3/2} \quad (30)$$

The intermolecular chain transfer rate coefficient was taken as 133 M^{-1} s^{-1} to match the work of Reyes and Asua.[30] Furthermore, the branching fractions for these cases were determined by adding the contribution of conventional backbiting, the (much smaller) contribution of long chain backbiting and the contribution of intermolecular chain transfer. In order to simplify the computation, the kMC simulations assumed that the FRP system had disproportionation as the termination mechanism. Although this was introduced to simplify the system, it had essentially no effect on the branching fraction.

As seen in Figure 10, the effect of these additional transfer reactions on differences between FRP and CRP is realtively low, particularly at lower conversions where the traditional backbiting dominates. At higher conversions there is a perceptible increase in the branching fraction due to the intermolecular transfer for both FRP and CRP. However, the extent of intermolecular transfer is small (below 30% of total fraction), as seen by the similarity between the branching fractions observed with and without these additional transfer reactions, which is consistent with the experiments of Charleux et al.[6] Importantly, the trends are the same for the cases with and without these additional transfer reactions, indicating that the conclusions derived for the systems with exclusive backbiting also hold for systems which explicitly account for intermolecular transfer.

Chain Length Distribution and Branching Amount. Another advantage of kMC simulations is that they can be used to assess the characteristics of each polymer chain as well as looking at the average properties of the polymer. Figure 11 shows the distribution of number of chains as a function of the degree of polymerization and also the number of branches per chain.

This is a simulation for a typical ATRP process, with target DP 200. As can be seen under the conditions used or the simulation, the majority of chains have 0, 1, or 2 branches, and chains with 3 or more branches amount to about 20% of all chains. Furthermore, due to presence of interchain transfer, it is possible to have multiple propagating sites on a single polymer. Therefore, if the acrylate is used as a macroinitiator, there will be a fraction of complex star like material, in addition to the component of block copolymer.

Analytic Solution for Branching Fraction. A simple analysis of the reactions critical for branching in radical polymerization gives the following differential equations for monomer conversion, formation of tertiary radicals and the corresponding dormant species, and for formation of branches:

$$\frac{d[M]}{dt} = k_p[P^\bullet][M] - k_{p3}[P_3^\bullet][M] \tag{31}$$

$$\begin{aligned}\frac{d[P_3^\bullet]}{dt} = {} & k_{bb}([P^\bullet] - [P(1)^\bullet] - [P(2)^\bullet]) - k_{p3}[P_3^\bullet][M] \\ & + k_{trp}[P^\bullet]([M]_0 - [M]) + k_{a3}[P_3X][CuX] \\ & - k_{d3}[P_3^\bullet][CuX_2] - k_t[P_3^\bullet][P^\bullet] - k_t[P_3^\bullet][P_3^\bullet]\end{aligned} \tag{32}$$

$$\frac{d[P_3X]}{dt} = -k_{a3}[P_3X][CuX] - k_{d3}[P_3^\bullet][CuX_2] \tag{33}$$

$$\frac{d[B]}{dt} = k_{p3}[P_3^\bullet][M] \tag{34}$$

where $[M]$ and $[M]_0$ are instantaneous and initial concentrations of monomer, $[P^\bullet]$, $[P(1)^\bullet]$, and $[P(2)^\bullet]$ are the concentrations of the secondary radicals: total and of short chains, DP = 1 and 2, respectively, and $[P_3^\bullet]$ is the concentration of tertiary radicals; $[P_3X]$ and $[B]$ denote the concentrations of the tertiary dormant species and of branches (branching points), respectively. $[CuX]$ and $[CuX_2]$ denote the concentrations of the activator and deactivator complexes.

Combining eqs 32−34, one gets the differential equations for kinetics of accumulation of the sum of branches and tertiary species:

$$\begin{aligned}\frac{d([B] + [P_3X] + [P_3^\bullet])}{dt} = {} & k_{bb}([P^\bullet] - [P(1)^\bullet] - [P(2)^\bullet]) \\ & + k_{trP}[P^\bullet]([M]_0 - [M]) \\ & - k_t[P_3^\bullet][P^\bullet] - k_t[P_3^\bullet][P_3^\bullet]\end{aligned} \tag{35}$$

Experimental data indicate that in most of radical polymerizations of acrylates the rate of termination is significantly lower than the rate of transfer (several branches on one terminated chain in FRP and the proportion of transfer events to the termination events in CRP much larger than unity and the average DP of propagating radicals much higher than 1). Taking this into account, the termination terms and those with short chain radicals of eq 35 can be neglected:

$$\begin{aligned}\frac{d([B] + [P_3X] + [P_3^\bullet])}{dt} = {} & k_{bb}[P^\bullet] \\ & + k_{trP}[P^\bullet]([M]_0 - [M])\end{aligned} \tag{36}$$

Combining eqs 31 and 36, one gets the following equation:

$$\frac{d([B] + [P_3X] + [P_3^\bullet])}{d[M]} = -\frac{k_{bb}[P^\bullet] + k_{trP}[P^\bullet]([M]_0 - [M])}{k_p[P^\bullet][M] + k_{p3}[P_3^\bullet][M]} \tag{37}$$

Assuming the tertiary propagation is slower than the secondary propagation, one gets

$$\begin{aligned}\frac{d([B] + [P_3X] + [P_3^\bullet])}{d[M]} &= -\frac{k_{bb}[P^\bullet] + k_{trP}[P^\bullet]([M]_0 - [M])}{k_p[P^\bullet][M]} \\ &= \frac{k_{bb} + k_{trP}[M]_0}{k_p[M]} + \frac{k_{trP}}{k_p}\end{aligned} \tag{38}$$

and consequently

$$\begin{aligned}&([B] + [P_3X] + [P_3^\bullet]) \\ &\quad = -\int_{[M]_0}^{[M]} \left(\frac{k_{bb} + k_{trP}[M]_0}{k_p[M]} - \frac{k_{trP}}{k_p}\right) d[M]\end{aligned} \tag{39}$$

This equation has an analytical solution:

$$\begin{aligned}&([B] + [P_3X] + [P_3^\bullet]) \\ &\quad = \frac{k_{bb} + k_{trP}[M]_0}{k_p} \log\left(\frac{[M]_0}{[M]}\right) - \frac{k_{trP}}{k_p}([M]_0 - [M])\end{aligned} \tag{40}$$

Equation 40 is a good approximation, if not too high conversion is reached and above assumptions are valid. At very high conversions almost all propagating species are tertiary ones, and consequently most of monomer addition occurs on tertiary radicals, making eq 39 invalid, as well as the final integration.

It is important that eqs 31−40 are valid for both CRP and FRP (for the latter the terms with dormant species and/or activator/deactivator (CuX/CuX_2) become equal to zero). This indicates that the lower branching density in CRP practically entirely stems (with the very infrequent exceptions of special cases of very low DP_n and very efficient termination, when the approximations adopted in derivation of eq 40 become invalid) from the presence of dormant tertiary species in CRP. When the concentration of dormant tertiary species P_3X ($\gg P_3^\bullet$) is of the same order of magnitude as the concentration of branching points B, then the branching density is significantly lower in CRP in comparison to FRP. In other words, if the theoretical maximum average number of branches in polymer of the given DP_n, stemming from the branching density of polymer obtained in FRP, is not higher than, say, 2, then it is a possibility to observe a significant decrease of branching in CRP (the number of branches can decrease by one when almost all dormant species are tertiary). When, however, one gets in CRP polymer of higher DP_n, for which the theoretical number of branching points is high, then the possible decrease of it by one does not decrease significantly the branching density.

Concluding, the results of the above analysis indicate that the equilibrium constants of the tertiary species deactivation/activation and/or dynamics of this equilibrium (determined by rate coefficients and concentrations of activator/deactivator) as well the rate of backbiting and propagation on tertiary radicals (determined by the rate coefficients and monomer concentration), together settle the distribution of entities of the sum of branching points and tertiary species. However, these competing processes, only together with DP_n of polymer, determine if branching in CRP is significantly lower than in FRP. A derivation is presented

in the Supporting Information, which gives a qualitative picture of how the various ATRP equilibrium constants and the relative concentrations of dormant species can give rise to reduced branching in acrylates.

CONCLUSIONS

Both Predici and kMC simulations illustrate that the branching fraction in ATRP (and in general in other CRP systems) of acrylates can be significantly lower than in FRP, depending on the ATRP catalyst properties and reaction conditions.

The concept of competing processes successfully explained the difference in branching fraction. It relies on the complex interaction of (i) the ATRP equilibrium between secondary propagating and dormant species, (ii) the ATRP equilibrium between tertiary propagating and dormant species, and (iii) the interconversion between secondary and tertiary radicals by transfer and tertiary propagation. These three processes interact with each other, which can delay the balancing of forward and backward rates in one or two of these processes. In general, as soon as the interconversion rates are balanced, the instantaneous branching fractions in ATRP are the same as for a typical FRP case. Moreover, if this balancing occurs at a sufficiently low conversion, the cumulative branching fraction of the ATRP will become almost identical to the FRP case.

In agreement with the recent results of Reyes and Asua, a fast tertiary deactivation is needed to reduce the fraction of branches in ATRP. In that case, the tertiary propagation rate is sufficiently lower than the transfer rate. However, simulations clearly show that also tertiary activation codetermines the branching fraction. For sufficiently high activation rate coefficients, branching fraction can be similar to the FRP case, even with rapid tertiary deactivation.

In addition to catalyst properties, reaction conditions determine to the extent of branching. The concentration of catalyst has a negligible effect on the branching fraction, since they affect all reaction rates in a similar way. Interestingly, both branching fractions in ATRP and FRP increased upon dilution, due to the unimolecular nature of the backbiting reaction. However, the concentration of initiator affects the branching fraction significantly, with higher initiator concentrations, i.e., lower targeted degrees of polymerization, giving lower branching fractions at a given conversion.

The kMC simulations showed minimal influence of chain length dependent rate coefficients on the branching fraction and that introducing intermolecular chain transfer leads to a small increase in the branching fraction, particularly at higher conversions. Finally, the analytical solution suggests that the lower branching density in polyacrylates prepared by ATRP essentially stems from the presence of dormant tertiary species.

Although this work has simulated the branching fractions for polyacrylates synthesized by ATRP, the method outlined here can easily be extended to other CRP methods such as NMP and RAFT polymerization. In all these three systems there is an equilibrium between dormant and active secondary and tertiary species and an interchange from secondary to tertiary via transfer and tertiary to secondary via addition of monomer. However, the roles of the activating and deactivating species are different for ATRP, NMP, and RAFT. In particular, for NMP the secondary and tertiary deactivation would occur with the nitroxide radical, not the CuX_2 catalyst, and there is no activator catalyst in NMP since activation occurs by direct bond homolysis. In this way the competitive processes scheme (Scheme 3) for branching in acrylates can be adapted to NMP by including these two reactions. Similarly, in RAFT polymerization the activation and deactivation of chains occur through the RAFT exchange process; therefore, the activating species is a propagating radical, and the deactivating species is the dithioester group. Therefore, the competitive processes can be used to explain the branching in RAFT polymerization by substituting halogen-capped species for dithioester species, CuX activators for propagating radicals, and CuX_2 deactivators for dithioester species.

ASSOCIATED CONTENT

Supporting Information. PREDICI simulations for the effect of CuX and CuX_2 on the rates and branching fraction, PREDICI simulations for the effect of dilution on the rates and branching fraction, additional MC simulations for the branching fraction, and scaling arguments to explain the branching phenomena in CRP. This material is available free of charge via the Internet at http://pubs.acs.org.

AUTHOR INFORMATION

Corresponding Author
*E-mail: km3b@andrew.cmu.edu.

ACKNOWLEDGMENT

The work was supported by the National Science Foundation (DMR 09-69301 and CHE 10-26060), The Polish Ministry of Science and Higher Education from the budget funds for science for years 2009−2012, The Fund for Scientific Research Flanders (FWO), the Interuniversity Attraction Poles Programme-Belgian State-Belgian Science Policy, and the Long Term Structural Methusalem Funding by the Flemish Government.

REFERENCES

(1) Flory, P. J. *J. Am. Chem. Soc.* **1937**, *59*, 241–253.
(2) (a) Matheson, M. S.; Auer, E. E.; Bevilacqua, E. B.; Hart, E. J. *J. Am. Chem. Soc.* **1949**, *71*, 2610–2617. (b) Roedel, M. J. *J. Am. Chem. Soc.* **1953**, *75*, 6110–6112. (c) Ehrlich, P.; Mortimer, G. *Adv. Polym. Sci.* **1970**, *7*, 386–448. (d) Hutchinson, R. A.; Richards, J. R.; Aronson, M. T. *Macromolecules* **1994**, *27*, 4530–4537.
(3) (a) Aggarwal, S. L.; Sweeting, O. J. *Chem. Rev.* **1957**, *57*, 665–742. (b) White, J. L.; Dharod, K. C.; Clark, E. S. *J. Appl. Polym. Sci.* **1974**, *18*, 2539–2568.
(4) (a) Lovell, P. A.; Shah, T. H.; Heatley, F. *Polym Commun* **1991**, *32*, 98–103. (b) Lovell, P. A.; Shah, T. H.; Heatley, F. *Polym. Mater. Sci. Eng.* **1991**, *64*, 278.
(5) Junkers, T.; Barner-Kowollik, C. *J. Polym. Sci., Part A: Polym. Chem.* **2008**, *46*, 7585–7605.
(6) Farcet, C. l.; Belleney, J. l.; Charleux, B.; Pirri, R. *Macromolecules* **2002**, *35*, 4912–4918.
(7) Yu-Su, S. Y.; Sun, F. C.; Sheiko, S. S.; Konkolewicz, D.; Lee, H.-i.; Matyjaszewski, K. *Macromolecules* **2011**.
(8) (a) Liang, K.; Hutchinson, R. A. *Macromol. Rapid Commun.* **2011**, *32*, 1090–1095. (b) Liang, K.; Hutchinson, R. A.; Barth, J.; Samrock, S.; Buback, M. *Macromolecules* **2011**.
(9) (a) Chiefari, J.; Jeffery, J.; Mayadunne, R. T. A.; Moad, G.; Rizzardo, E.; Thang, S. H. *Macromolecules* **1999**, *32*, 7700–7702. (b) Junkers, T.; Barner-Kowollik, C. *Macromol. Theory Simul.* **2009**, *18*, 421–433.
(10) Peck, A. N. F.; Hutchinson, R. A. *Macromolecules* **2004**, *37*, 5944–5951.

(11) (a) Ahmad, N. M.; Heatley, F.; Lovell, P. A. *Macromolecules* **1998**, *31*, 2822–2827. (b) Castignolles, P.; Graf, R.; Parkinson, M.; Wilhelm, M.; Gaborieau, M. *Polymer* **2009**, *50*, 2373–2383. (c) Junkers, T.; Koo, S. P. S.; Davis, T. P.; Stenzel, M. H.; Barner-Kowollik, C. *Macromolecules* **2007**, *40*, 8906–8912. (d) Yu, Y.; DesLauriers, P. J.; Rohlfing, D. C. *Polymer* **2005**, *46*, 5165–82. (e) Pollard, M.; Klimke, K.; Graf, R.; Spiess, H. W.; Wilhelm, M.; Sperber, O.; Piel, C.; Kaminsky, W. *Macromolecules* **2004**, *37*, 813–825.

(12) (a) Gaborieau, M.; Koo, S. P. S.; Castignolles, P.; Junkers, T.; Barner-Kowollik, C. *Macromolecules* **2010**, *43*, 5492–5495. (b) Parkinson, M.; Klimke, K.; Spiess, H. W.; Wilhelm, M. *Macromol. Chem. Phys.* **2007**, *208*, 2128–2133.

(13) Shroff, R. N.; Mavridis, H. *Macromolecules* **1999**, *32*, 8454–8464.

(14) (a) Wood-Adams, P. M.; Dealy, J. M.; deGroot, A. W.; Redwine, O. D. *Macromolecules* **2000**, *33*, 7489–7499. (b) Gaborieau, M.; Nicolas, J.; Save, M.; Charleux, B.; Vairon, J.-P.; Gilbert, R. G.; Castignolles, P. *J. Chromatogr. A* **2008**, *1190*, 215–223.

(15) Wood-Adams, P. M.; Dealy, J. M. *Macromolecules* **2000**, *33*, 7481–7488.

(16) Hlalele, L.; Klumperman, B. *Macromolecules* **2011**, *44*, 5554–5557.

(17) (a) Asua, J. M.; Beuermann, S.; Buback, M.; Castignolles, P.; Charleux, B.; Gilbert, R. G.; Hutchinson, R. A.; Leiza, J. R.; Nikitin, A. N.; Vairon, J.-P.; van Herk, A. M. *Macromol. Chem. Phys.* **2004**, *205*, 2151–2160. (b) Barner-Kowollik, C.; Günzler, F.; Junkers, T. *Macromolecules* **2008**, *41*, 8971–8973. (c) Reyes, Y.; Arzamendi, G.; Asua, J. M.; Leiza, J. R. *Macromolecules* **2011**, *44*, 3674–3679.

(18) (a) Goto, A.; Fukuda, T. *Prog. Polym. Sci.* **2004**, *29*, 329–385. (b) Braunecker, W. A.; Matyjaszewski, K. *Prog. Polym. Sci.* **2007**, *32*, 93–146.

(19) (a) Georges, M. K.; Veregin, R. P. N.; Kazmaier, P. M.; Hamer, G. K. *Macromolecules* **1993**, *26*, 2987–8. (b) Hawker, C. J.; Bosman, A. W.; Harth, E. *Chem. Rev.* **2001**, *101*, 3661–3688.

(20) (a) Wang, J.-S.; Matyjaszewski, K. *J. Am. Chem. Soc.* **1995**, *117*, 5614–15. (b) Kato, M.; Kamigaito, M.; Sawamoto, M.; Higashimura, T. *Macromolecules* **1995**, *28*, 1721–3. (c) Matyjaszewski, K.; Xia, J. *Chem. Rev.* **2001**, *101*, 2921–2990.

(21) (a) Chiefari, J.; Chong, Y. K.; Ercole, F.; Krstina, J.; Jeffery, J.; Le, T. P. T.; Mayadunne, R. T. A.; Meijs, G. F.; Moad, C. L.; Moad, G.; Rizzardo, E.; Thang, S. H. *Macromolecules* **1998**, *31*, 5559–5562. (b) Perrier, S.; Takolpuckdee, P. *J. Polym. Sci., Part A: Polym. Chem.* **2005**, *43*, 5347–5393.

(22) Szwarc, M. *Nature* **1956**, *178*, 1168–9.

(23) Moad, G.; Rizzardo, E.; Thang, S. H. *Aust. J. Chem.* **2005**, *58*, 379–410.

(24) Tsarevsky, N. V.; Matyjaszewski, K. *Chem. Rev.* **2007**, *107*, 2270–2299.

(25) di Lena, F.; Matyjaszewski, K. *Prog. Polym. Sci.* **2010**, *35*, 959–1021.

(26) Ahmad, N. M.; Charleux, B.; Farcet, C.; Ferguson, C. J.; Gaynor, S. G.; Hawkett, B. S.; Heatley, F.; Klumperman, B.; Konkolewicz, D.; Lovell, P. A.; Matyjaszewski, K.; Venkatesh, R. *Macromol. Rapid Commun.* **2009**, *30*, 2002–2021.

(27) D'hooge, D. R.; Reyniers, M.-F.; Stadler, F. J.; Dervaux, B.; Bailly, C.; Du Prez, F. E.; Marin, G. B. *Macromolecules* **2010**, *43*, 8766–8781.

(28) Matyjaszewski, K.; Woodworth, B. E. *Macromolecules* **1998**, *31*, 4718–4723.

(29) Matyjaszewski, K. *Macromolecules* **1998**, *31*, 4710–4717.

(30) Reyes, Y.; Asua, J. M. *Macromol. Rapid Commun.* **2011**, *32*, 63–67.

(31) Tsarevsky, N. V.; Braunecker, W. A.; Vacca, A.; Gans, P.; Matyjaszewski, K. *Macromol. Symp.* **2007**, *248*, 60–70.

(32) Matyjaszewski, K. *Macromolecules* **2002**, *35*, 6773–6781.

(33) Tang, W.; Kwak, Y.; Braunecker, W.; Tsarevsky, N. V.; Coote, M. L.; Matyjaszewski, K. *J. Am. Chem. Soc.* **2008**, *130*, 10702–10713.

(34) Seeliger, F.; Matyjaszewski, K. *Macromolecules* **2009**, *42*, 6050–6055.

(35) (a) Smith, G. B.; Russell, G. T.; Heuts, J. P. A. *Macromol. Theory Simul.* **2003**, *12*, 299–314. (b) Johnston-Hall, G.; Monteiro, M. J. *J. Polym. Sci., Part A: Polym. Chem.* **2008**, *46*, 3155–3173. (c) Theis, A.; Davis, T. P.; Stenzel, M. H.; Barner-Kowollik, C. *Macromolecules* **2005**, *38*, 10323–10327. (d) Vana, P.; Davis, T. P.; Barner-Kowollik, C. *Macromol. Rapid Commun.* **2002**, *23*, 952–956.

(36) D'hooge, D. R.; Reyniers, M.-F.; Marin, G. B. *Macromol. React. Eng.* **2009**, *3*, 185–209.

(37) Kothe, T.; Marque, S.; Martschke, R.; Popov, M.; Fischer, H. *J. Chem. Soc., Perkin Trans. 2* **1998**, 1553–1559.

(38) (a) Junkers, T.; Theis, A.; Buback, M.; Davis, T. P.; Stenzel, M. H.; Vana, P.; Barner-Kowollik, C. *Macromolecules* **2005**, *38*, 9497–9508. (b) Theis, A.; Feldermann, A.; Charton, N.; Stenzel, M. H.; Davis, T. P.; Barner-Kowollik, C. *Macromolecules* **2005**, *38*, 2595–2605.

(39) Bawn, C. E. H.; Verdin, D. *Trans. Faraday Soc.* **1960**, *56*, 815–822.

(40) (a) Moad, G.; Rizzardo, E.; Solomon, D. H.; Johns, S. R.; Willing, R. I. *Makromol. Chem., Rapid Commun.* **1984**, *5*, 793–798. (b) Buback, M.; Huckestein, B.; Kuchta, F.-D.; Russell, G. T.; Schmid, E. *Macromol. Chem. Phys.* **1994**, *195*, 2117–2140.

(41) Plessis, C.; Arzamendi, G.; Alberdi, J. M.; van Herk, A. M.; Leiza, J. R.; Asua, J. M. *Macromol. Rapid Commun.* **2003**, *24*, 173–177.

(42) Arzamendi, G.; Plessis, C.; Leiza, J. R.; Asua, J. M. *Macromol. Theory Simul.* **2003**, *12*, 315–324.

(43) Szymanski, R. *e-Polym.* **2009**, *no. 44*, xxxx.

(44) Gillespie, D. T. *J. Phys. Chem.* **1977**, *81*, 2340.

(45) Heuts, J. P. A.; Russell, G. T. *Eur. Polym. J.* **2006**, *42*, 3–20.

(46) Jacobson, H.; Stockmayer, W. H. *J. Chem. Phys.* **1950**, *18*, 1600.